Aerodynamic Design of Inward-Turning Inlets with Shape Transition

Aerodynamic design of inward-turning inlets with shape transition

Cite as: AIP Conference Proceedings **2293**, 200019 (2020); https://doi.org/10.1063/5.0026542
Published Online: 25 November 2020

Bing Xiong, Michele Ferlauto, and Xiaoqiang Fan

Aerodynamic Design of Inward-Turning Inlets with Shape Transition

Bing Xiong[1], Michele Ferlauto[2,a)] and Xiaoqiang Fan[1]

[1]*College of Aerospace Science and Engineering, National University of Defense Technology, Changsha, China*
[2]*Department of Mechanical and Aerospace Engineering, Politecnico di Torino, Turin, Italy*

[a)]Corresponding author: michele.ferlauto@polito.it

Abstract. Rectangular-to-Ellipse Shape Transition (REST) inlets are a kind of inward-turning inlets designed for hypersonic vehicles, especially under integration design backgrounds. The streamline tracing technique is an inverse method for designing inward-turning inlets by extracting different streamtubes from the same reference flow. In present work, the streamline tracing technique is coupled with an optimization procedure. The procedure for designing a REST inlet with prescribed mass capture at the design point and optimal performance is illustrated.

INTRODUCTION

The air-breathing hypersonic vehicle is a critical item for access to the space in Single-Stage-To-Orbit (SSTO) or Two-Stage-To-Orbit (TSTO), and the primary choice for the propulsion system is the scramjet [1, 2]. Inward-turning inlet for that systems can be generated accurately by using streamline tracing techniques [3, 4]. Three-dimensional inward-turning inlets [3] stand out from many other types of hypersonic inlets because of its high compression efficiency and good mass capture performance [5]. As a result, it is considered the best choice for a scramjet. In practical applications, inward-turning inlets are easily integrated with the vehicle airframe [6], as well as with ramjet/scramjet combustors having circular or elliptical inlet sections [7, 8]. However, the entrance shape and the exit shape cannot be controlled at the same time. To solve this problem, a method of shape transition was proposed. Smart *et al.* [7] firstly designed an inward-turning inlet with a Rectangular-to-Ellipse Shape Transition (REST). The adopted streamline tracing technique is a kind of inverse method [9, 10] for designing inward-turning inlets by extracting different streamtubes from the same reference flow. The REST inlet was generated with a combination of two inlets which were traced through a reversed nozzle flowfield. In previous studies, optimization methodology has been used with the aim of improving the performances of inlets traced through this basic flowfield [11]. In our work, the optimization procedure was directly coupled to the design of the REST inlet.

MATHEMATICAL MODEL

Parameterization

Essentially, an inward-turning inlet is the envelope of streamtubes extracted from a basic flowfield. The inlet performances are therefore significantly affected by this basic field, represented schematically in Figure 1 . As shown in this figure, the inflow is mainly compressed by the conical shock and then by the reflected shock. A cylindrical center-body is installed on the symmetry axis in order to avoid the presence of a Mach disk which may lead to large total pressure losses [12]. In order to optimize the inward-turning inlet, a parameterization should be accomplished firstly. Figure 2 illustrates the parameterization methodology of a basic flowfield. Properties of the basic flowfield are mainly determined by the shape of compression wall which is shown in red line in Figure 2. The total length of basic flowfield is L_t, and the cowl lip is located at point D (L_c). The compression wall CH is divided into two segments at point E. Line CE represents the external compression of the inflow, whereas line EH represents the internal

International Conference of Numerical Analysis and Applied Mathematics ICNAAM 2019
AIP Conf. Proc. 2293, 200019-1–200019-4; https://doi.org/10.1063/5.0026542
Published by AIP Publishing. 978-0-7354-4025-8/$30.00

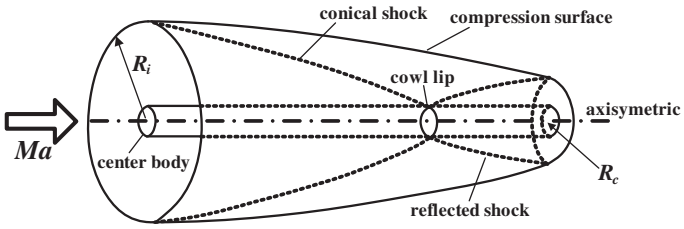

FIGURE 1. A typical axisymmetric basic flowfield.

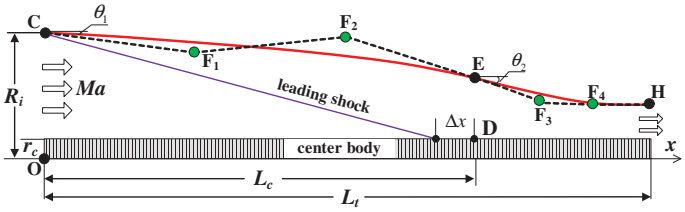

FIGURE 2. Parameterization of the basic flowfield.

compression. Each line is generated using a third order Quasi-Uniform B-Spline (QUBS) curve [13] which has four control points. For the basic flowfield, the entrance radius R_i is set as reference length. All lengths have been therefore normalized by R_i throughout the present paper. As shown in Figure 2, the distance between the incident point and the cowl lip is $|\Delta x|$, which is in turn related to the mass capture capability of the intake. The optimal condition is the so-called "shock-on-lip" configuration where the leading shock is perfectly incident on the cowl lip, that is $|\Delta x| = 0$. Each flexible point (green color) has two degree of freedom, namely the coordinate pairs (x, r). Many key features of basic flowfield depend on these control points, e.g. the constriction ratios, shock angle, etc.

Streamline tracing and shape transition

Once the basic flowfield has been computed, inward-turning inlets can be generated by applying the streamline tracing technique. The streamline tracing technique is applied in the streamwise direction, when the entrance shape of the inlet is specified, and along the opposite direction, when the intake shape is set at the exit section. A typical basic flowfield we obtained is presented in Figure 3(a). The design point is characterized by an incoming flow having Mach number M_i=6.0, pressure p_i=2549.2 Pa and temperature T_i=226 K. A REST inlet is a kind of inlet which has a rectangular-like entrance and an elliptical exit. An inward turning inlet can be generated through the basic flowfield if the Flow Capture Shape (FCT) is set. Figure 3(b) illustrates how an inward-turning inlet is extracted from the basic flowfield. To this streamtraced solution we assigned the name *shape A*. The 3D inlet leading edge location fits perfectly with the shock surface. Thus the inviscid inlet is able to capture the full mass prescribed at design conditions. This inlet has the entrance shape assigned by the designer, whereas the exit shape cannot be controlled, since it is the result

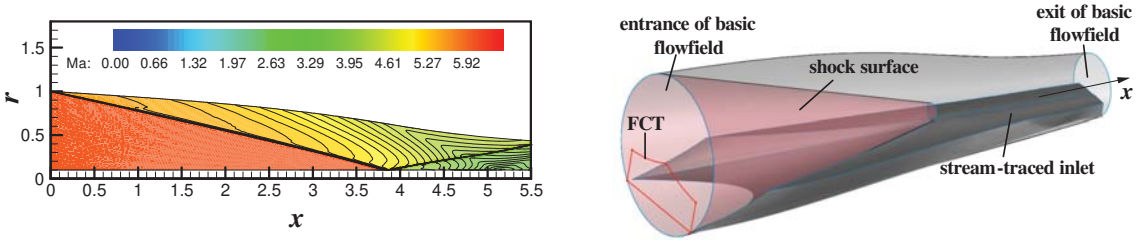

(a) (b)

FIGURE 3. Mach contours on the axisymmetric basic flowfield (a) and a sketch of the stream-traced inlet (b).

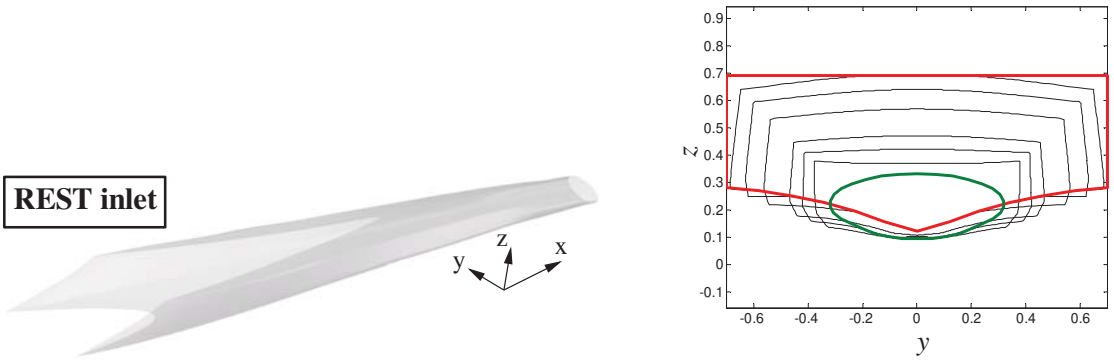

(a) (b)

FIGURE 4. 3D view of the final REST inlet geometry (a). Plot of cross-section of the inlet along the x-axis (b).

of the streamtracing procedure. Therefore the procedure is applied in a similar fashion by setting at the intake exit a prescribed shape and area, e.g. an elliptical one, and by tracing a streamtube backwards. This second intake solution is named *shape B*. The geometry of the REST inlet is obtained as a combination of shape A and B by applying an integration function as suggested in Ref. [7]. The two inlets do not have anyway the same area distribution along the axial coordinate x, owing to the non-uniform compression of the basic flowfield. To make sure the REST inlet has the same area distribution as shape A, shape scaling was applied at each intermediate cross section. The procedure to control the cross-section area distribution by shape scaling was illustrated in Ref. [7]. The final REST inlet model as well as several cross-section shapes along the axial direction are presented in Figure 4.

Optimization procedure

As illustrated in Figure 2, the geometry of the basic flowfield is expressed by using several parameters. In the primary optimization, constriction ratios of basic flowfield are fixed so that the inlet constriction ratios will not far from the fixed value. In order to reduce the computational cost of the optimization, additional constraints to the control points have been introduced. Control points F1, F2, and F4 are respectively put in the tripartite position of each curve, and the direction of the exit flow has been set as horizontal. As a result, there are only three free parameters left, namely $\boldsymbol{X} = [r_{F1}, r_{F2}, x_{F4}]^T$. Actually, we can choose another optimization vector $\boldsymbol{X} = [\theta_1, \theta_2, x_{F4}]^T$ which is more physically meaningful. In addition, we set a range for each parameter by considering a trade-off between time-saving and flexibility. For a compression system, the total pressure recovery is of great significance for the engine thrust. Therefore, the total pressure recovery coefficient of the inlet is selected as an optimization objective. In present work, we use the predicted total pressure recovery $\sigma_p = \sqrt{\sigma_A^2 + \sigma_B^2}$ as objective. Furthermore, the inlet mass capture should meet engine requirements. For this kind of inward-turning inlet, the leading shock of the basic flowfield has great effects on the mass capture performance. In the basic flowfield shown in Figure2, the smaller $|\Delta x|$ is, the higher the mass capture performance an inlet will be. Therefore, $|\Delta x|$ is another optimization objective of this work. We gave an additional constraint of $|\Delta x|/L_t \leq 1\%$, which means that a basic flowfield will be regarded as realistic only when the parameter meets this constraint. Finally, the optimization problem is expressed as follows

$$\min(-\sigma_p, |\Delta x|) \tag{1}$$

$$\text{s.t.} \begin{cases} 0 \leq \theta_1 \leq 13^o \\ 0 \leq \theta_2 \leq 20^o \\ 0 \leq \theta_1 \leq 13^o \\ (2x_E + x_H)/3 < x_{F4} < x_H \\ !\Delta x|/L_t < 1.0\% \end{cases} \tag{2}$$

This optimization procedure was realized by using the ISIGHT software suite, which is an efficient tool for combining different software and programs together to achieve automation of parameterization, simulation, and optimization. The NSGA-II optimization algorithm was adopted to solve the constrained optimum problem.

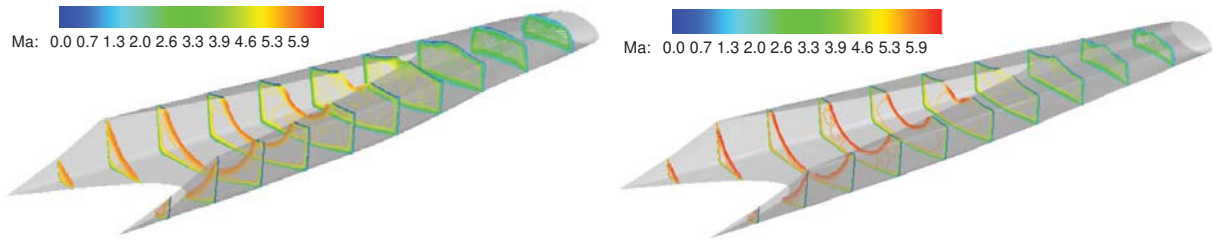

(a) (b)

FIGURE 5. Intake geometry and Mach contours for the final viscous solution for Cfg-1 (a) and Cfg-2 (b).

NUMERICAL RESULTS

The optimization process identifies a set of optimal solutions. A Pareto front can be also drawn. From the latter, we extracted here two solutions, namely Cfg-1 and Cfg-2, as an example. The optimality of the inviscid results obtained are confirmed by RANS-based CFD validations [14] reported in Figure 5. As visible, from the analysis of the flowfield at design conditions, no flow separations occur. With respect to the inviscid solution, in the viscous case the shock surface does not fit perfectly with the 3-D leading edge, thus leading to a flow spillage. Mass capture ratios for Cfg-1 and Cfg-2 decreases to the 98.3% and 97.5% respectively. By inviscid computations we obtain that the total pressure recovery of Cfg-1 is improved by 4.28% through the optimization. For the viscous results, the total pressure performance of Cfg-1 is improved by 6.83%, but with lower mass capture ratio. From this perspective, we concluded that the inviscid procedure is still able to improve the REST inlet performances during the optimization process.

CONCLUSIONS

A numerical procedure for the optimal design of REST inlets has been proposed. Results show that a REST inlet can be well represented parametrically with a reduced set of variables then used as control parameters in the optimization procedure. The optimization performed at design point have shown to improve the performances under off-design conditions. Improvements decrease with decreasing inflow Mach numbers owing to the weaker shocks involved.

ACKNOWLEDGMENTS

The authors gratefully acknowledge the supports of the NSFC (Nos. 11572347 and 11872071) and the China Scholarship Council (CSC). Computational resources were provided by hpc@polito.it, a project of Academic Computing within the Department of Control and Computer Engineering at the Politecnico di Torino.

REFERENCES

[1] F. Billig, R. Baurle, and C. Tam, 9th Int. Space Planes and Hyp. Sys. and Tech. Conf., Norfolk, VA (1999).
[2] A. Kuranov and A. Korabelnikov, Journal of Propulsion and Power **24**, 1229–1247 (2008).
[3] A. Kothari, C. Tarpley, and T. McLaughlin, 32nd Joint Propulsion Conf., Buena Vista, FL (1996).
[4] Y. You, 17th AIAA Int. Space Planes and Hyp. Sys. and Tech. Conf., San Francisco, CA (2011).
[5] X. He, Z. Zhou, S. Qin, and F. Wei, Chinese Journal of Aeronautics **29**, 1–8 (2016).
[6] J. Liu, F. Ding, W. Huang, and L. Jin, Acta Astronautica **102**, 81–88 (2014).
[7] M. Smart, Journal of Propulsion and Power **15**, 408–416 (1999).
[8] E. Degregori *et al.* , AIP Conference Proceedings **1978**, p. 470114 (2018).
[9] M. Ferlauto, Inverse Problems in Science and Engineering **23**, 798–817 (2015).
[10] M. Ferlauto and R. Marsilio, Computer & Fluids **35**, 304–325 (2006).
[11] J. Wang, J. Cai, T. Duan, and Y. Tian, Aerospace Science and Technology **66**, 44–58 (2017).
[12] H. Hornung, Journal of Fluid Mechanics **409**, p. 112 (2000).
[13] X. He and P. Shi, Journal of Nonparametric Statistics **3**, 299–308 (1994).
[14] B. Xiong, *et al.*, 5th ECCOMAS Young Investigators Conf., Krakow, Poland (2019)
.